

Electrochemical and Theoretical Studies of Novel Synthesized Benzimidazole Derivatives as Corrosion Inhibitors for Carbon Steel in 1 M HCl

Y. El Aoufir,^{1,2} Y. El Bakri,³ A. Chaouiki,^{2,4} H. Lgaz,² H. Oudda,²
R. Salghi,^{4,*} A. Guenbour¹ and E. M. Essassi³

¹Laboratory of Nanotechnology, Materials & Environment, Faculty of Sciences, University Mohammed V, Rabat, Morocco

²Laboratory Separation Processes, Faculty of Sciences, University Ibn Tofail, P.O. Box 242, Kenitra, Morocco

³Laboratory of Heterocyclic Organic Chemistry, URAC 21, Pole of pharmacochimie competence, Université Mohammed V, Faculty of Sciences, Rabat, Morocco

⁴Laboratory of Environmental Engineering and Biotechnology, ENSA, University Ibn Zohr, P.O. Box 1136, 80000 Agadir, Morocco

*Corresponding author: r.salghi@uiz.ac.ma

Received 18/03/2018; accepted 08/08/2020
<https://doi.org/10.4152/pea.202102105>

Abstract

New corrosion inhibitors of benzimidazole derivatives, namely, 6-methoxy-2-(((4-methoxy-3,5-dimethylpyridin-2-yl)methyl)sulfinyl)-1-vinyl-1H-benzo[d]imidazole (EMSB), 6-Methoxy-2-(((4-methoxy-3,5-dimethylpyridin-2-yl)methyl)) sulfinyl)-1-(prop-2-yn-1-yl)-1H benzimidazole (MSVB) and 6-methoxy-2-(((4-methoxy-3,5-dimethylpyridin-2-yl)methyl)sulfinyl)-1-(phenacyl)-1H benzimidazole (MSBP), have been synthesized. Their inhibiting action on the carbon steel corrosion in an acidic medium (1 M HCl) has been investigated by various corrosion monitoring techniques, such as weight loss measurement, potentiodynamic polarization, adsorption, electrochemical impedance spectroscopy (EIS) and basic computational calculations. The results of the investigation show that the inhibition efficiency of all the three inhibitors increases with higher inhibitors concentration, and decreases with a rise in temperature. The inhibitors, MSBP, MSVP and EMSB, show a corrosion inhibition efficiency of 98, 97 and 93%, respectively (dosage of 1×10^{-3} M). EIS measurements showed an increase in the transfer resistance with the inhibitors concentration. Polarization studies showed that the studied inhibitors are of the mixed type in nature. The adsorption of benzimidazole is described by the Langmuir isotherm. In addition, density functional theory (DFT), calculations and Molecular Dynamics simulations (MD) were undertaken to describe the electronic and adsorption properties of the synthesized inhibitors, including the synergistic/dispersive interactive effects of the multiple adsorptions of the various active constituents in the inhibitor film. Also, DFT and MD simulations were employed to support the experimental findings.

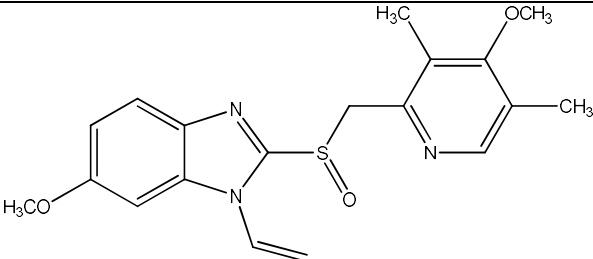
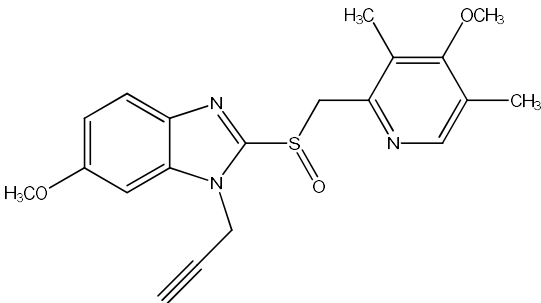
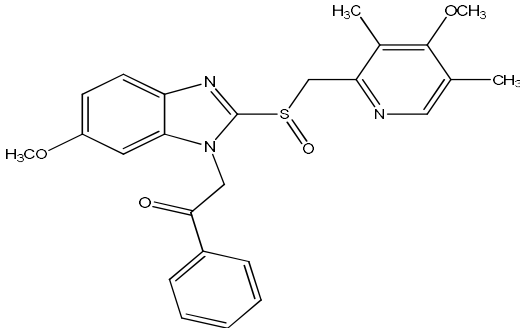
Keywords: Inhibition; carbon steel; Benzimidazole derivatives; acidic solutions; DFT; Molecular Dynamic.

Introduction

Metallic corrosion has been one of the most important problems facing steel in a wide range of fields, especially in engineering and industrial processes¹⁻³. By definition, metallic corrosion is basically a natural process which leads to the deterioration of substances, by means of chemical or electrochemical action, when they are exposed to harsh environments, which significantly reduces the most thermodynamically stable minerals which they are extracted from, such as oxides, carbonates, sulfides, etc.^{2,4} In fact, there are many industrial processes that require the application of acidic solutions, e.g., oil well acidization and acid pickling processes. For this purpose, chloride and sulfuric acid solutions are very often used. On the other hand, recent developments in the industrial sector have led to a renewed interest in carbon steel as the most popular metal that is commonly used in these industrial applications, due to its high mechanical strength, extreme thermal stability and exceptionally low cost. Inevitably, the employed acidic solutions during a wide range of applications certainly cause severe corrosion damage, property deterioration of related infrastructures and even enormous economic loss. Therefore, it is urgently needed to find a simple method for preventing or minimizing such type of adverse effects on metallic surfaces. In this context, among the available methods of corrosion protection, the use of inhibitors is one of the most practical methods, especially in an acidic solution. Also, this approach is an alternative technique that has the ability to reduce the economic effect, i.e. it is the most inexpensive solution against the aggressive effects of metallic corrosion. Today, many studies have been made on the corrosion inhibition of carbon steel in acidic media, by using organic corrosion inhibitors, which are the best candidates to prevent metallic corrosion, due to their environmental characteristics, low cost, and high efficiency. Up to now, the research has tended to focus on the class of organic inhibitors which contain π bonds, phenyl rings, an electron donating functional group, conjugated double bonds, heteroatoms (N, S, O, P), etc.⁵⁻⁷. These organic compounds can be adsorbed onto the metal surface, forming a protective film (chemical and/or physical adsorption). The adsorbed film blocks the corrosion cells on the metal surface and reduces the harmful attack of the corrosive medium. In this context, several researches have been carried out to study the inhibition properties of benzimidazole molecules and its effect on carbon steel corrosion inhibition⁸⁻¹⁵. Furthermore, we found that the inhibition efficiency depends on both the electronic and chemical structures (molecular area and satiric distribution of the substituents) of the molecules. Further, benzimidazole is a heterocyclic compound with a bicyclic structure consisting of the fusion of benzene and imidazole rings. Some derivatives of benzimidazole have been demonstrated as excellent inhibitors for carbon steel in acidic media^{16,17}. In this frame of reference, the anti-corrosion effect of the new benzimidazole has been investigated using both experimental and theoretical approaches. The present paper reports the inhibition effect of three new benzimidazole derivatives, namely 6-methoxy-2-(((4-methoxy-3,5-dimethylpyridin-2-yl)methyl)sulfinyl)-1-vinyl-1H-benzo[d]imidazole (EMSB), 6-Methoxy-2-(((4-methoxy-3,5-

dimethylpyridin-2-yl)methyl)sulfinyl)-1-(prop-2-yn-1-yl)-1H benzimidazole(MSVB) and 6-methoxy-2-(((4-methoxy-3,5-dimethylpyridin-2-yl)methyl)sulfinyl)-1-(phenacyl)-1-H-benzimidazole (MSBP). The molecular structures of the investigated compounds are shown in Table 1. The behavior of carbon steel in 1.0 M HCl, with and without inhibitors, was studied using Electrochemical Impedance Spectroscopy (EIS), Weight Loss measures (WL), as well as Potentiodynamic Polarization (PDP) techniques. The thermodynamic parameters for the adsorption process and the activation parameters for steel dissolution were determined and discussed. Density Functional Theory (DFT) and Molecular Dynamics (MD) simulation were used to study the correlation between the molecular properties of the studied inhibitors and their inhibition performance. Furthermore, the surface morphology of the inhibited and uninhibited C-steel specimens was investigated by a Scanning Electron Microscope (SEM).

Table 1. Abbreviation and chemical structures of the studied inhibitors.

Abbreviation	Structural formula
EMSB (by1)	 <p>6-methoxy-2-(((4-methoxy-3,5-dimethylpyridin-2-yl)methyl)sulfinyl)-1-vinyl-1H-benzo[d]imidazole</p>
MSVB (by2)	 <p>6-Methoxy-2-(((4-methoxy-3,5-dimethylpyridin-2-yl)methyl)sulfinyl)-1-(prop-2-yn-1-yl)-1H-benzimidazole (MSVB)</p>
MSBP (by3)	 <p>6-methoxy-2-(((4-methoxy-3,5-dimethylpyridin-2-yl)methyl)sulfinyl)-1-(phenacyl)-1-H-benzimidazole (MSBP)</p>

Experimental section

Inhibitors synthesis

6-Methoxy-2-(((4-methoxy-3,5-dimethylpyridin-2-yl)methyl)sulfinyl)-1-(prop-2-en-1-yl)-1H-benzimidazole (EMSB)

To a solution of 6-methoxy-2-(((4-methoxy-3,5-dimethylpyridin-2-yl)sulfinyl)-1H-benzo[d]imidazole (1 g, 2.89 mmol), in N,N-dimethylformamide (20 mL), there were added potassium carbonate (0.4 g, 2.89 mmol), propargyl bromide (0.43 mL, 2.89 mmol) and a catalytic amount of tetra n-butyammonium bromide. The reaction mixture was stirred for 12 h. The solution was then concentrated to dryness under reduced pressure, and the residue was extracted with dichloromethane. The precipitate formed by cooling was filtered and recrystallized from ethanol, to give crystals with a yield of 65%. The compound was characterized by N.M.R. ¹H-NMR (DMSO-d₆) (δ ppm): 2.31(s,3H,CH₃), 2.81(s,1H,CH), 3.83(s,3H;OCH₃), 6.93(d,1H,CH_{aromatique}), 7.48(d,1H,CH_{aromatique}) 8.41(s,1H,CH-N) ¹³C-NMR (DMSO-d₆) (δ ppm): 15.7(CH₃), 55.8(O-CH₃), 56.8(CH₂), 58.3(HC triple liaison), 61.7(C triple liaison C), 100.8(C_{aromatique}), 115(C-CH₃), 116.2(C_{aromatique}), 131.2(C-N) and 158.5(C=N).

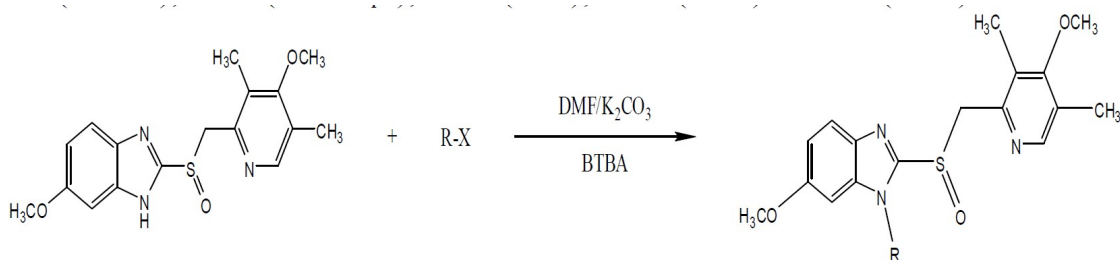
6-Methoxy-2-(((4-methoxy-3,5-dimethylpyridin-2-yl)methyl)sulfinyl)-1-(prop-2-yn-1-yl)-1H-benzimidazole (MSVB)

To a solution of 6-methoxy-2-(((4-methoxy-3,5-dimethylpyridin-2-yl)methyl)sulfinyl)-1-(prop-2-yn-1-yl)-1H-benzo[d]imidazole (1 g, 2.89 mmol), in N,N-dimethylformamide (20 mL), there were added potassium carbonate (0.4 g, 2.89 mmol), propargyl bromide (0.43 mL, 2.89 mmol) and a catalytic amount of tetra n-butyammonium bromide. The reaction mixture was stirred for 12 h. The solution was then concentrated to dryness under reduced pressure, and the residue was extracted with dichloromethane. The precipitate formed by cooling was filtered and recrystallized from ethanol, to give crystals with a yield of 65%. The compound was characterized by N.M.R. ¹H-NMR (DMSO-d₆) (δ ppm): 2.31(s,3H,CH₃), 2.81(s,1H,CH), 3.83(s,3H;O-CH₃), 6.93(d,1H,CH_{aromatique}), 7.48(d,1H,CH_{aromatique}) 8.41(s,1H,CH-N) ¹³C-NMR (DMSO-d₆) (δ ppm): 15.7(CH₃), 55.8(O-CH₃), 56.8(CH₂), 58.3(HC triple liaison), 61.7 (C triple liaison C), 100.8(C_{aromatique}), 115(C-CH₃), 116.2(C_{aromatique}), 131.2(C-N) and 158.5(C=N).

6-methoxy-2-(((4-methoxy-3,5-dimethylpyridin-2-yl)methyl)sulfinyl)-1-(phenacyl)-1-H-benzimidazole (MSBP)

To a solution of 6-methoxy-2-(((4-methoxy-3,5-dimethylpyridin-2-yl)methyl)sulfinyl)-1H-benzo[d]imidazole (1 g, 2.89 mmol), in N,N-dimethylformamide (20 mL), there were added potassium carbonate (0.4 g, 2.89 mmol), phenacyl bromide (2.89 mmol) and a catalytic amount of tetra n-butyammonium bromide. The reaction mixture was stirred for 12 h. The solution was then concentrated to dryness under reduced pressure, and the residue was extracted with dichloromethane. The precipitate formed by cooling was filtered and recrystallized from ethanol, to give a product with a yield of 60%. The compound was characterized by NMR. ¹H-NMR (DMSO-d₆) (δ ppm):

2.31(s,3H,CH₃), 2.81(s,1H,CH), 3.83(s,3H;O-CH₃), 6.22(s,2H,CH₂), 6.93(d,1H,CH_{aromatique}), 7.48(d,1H,CH_{aromatique}) 8.41(s,1H,CH-N) ¹³C-NMR (DMSO-d₆) (d ppm): 15.7(CH₃), 55.8(O-CH₃), 56.8(CH₂), 100.8(C_{aromatique}), 115(C-CH₃), 116.2(C_{aromatique}), 131.2(C-N), 158.5(C=N) and 190(C=O).



R = Allyl, Propargyl, Phenacyl

X = Br

General scheme

Materials and sample preparation

The carbon steel specimens, with a percentage chemical composition of 0.36 wt.% C, 0.66 wt.% Mn, 0.27 wt.% Si, 0.02 wt.% S, 0.015 wt.% P, 0.21 wt.% Cr, 0.02 wt.% Mo, 0.22 wt.% Cu, 0.06 wt.% Al and iron (remain), were used in all weight loss and electrochemical studies. Before exposing the specimens to the test solution, they were mechanically abraded and polished with 600, 800, 1000 and 1200 grade of emery paper, washed with double distilled water, followed by acetone, and finally dried at room temperature. The aggressive solutions (1 M HCl) were prepared by dilution of an analytical grade of 37% HCl with distilled water. The employed concentration range of inhibitors was from 10^{-6} to 10^{-3} M, and a solution without inhibitor was prepared for comparison. All solutions were prepared using distilled water. In addition, the potentiodynamic polarization technique was implemented by modifying temperatures from 303K to 333K, to examine the impact of temperature on the effectiveness of the tested inhibitors.

Weight loss tests

Identical coupons were immersed in 100 mL of an aggressive solution with different concentrations of inhibitors, at 303 K, for 6 h. The specimens of the used carbon steel had a rectangular form (length = 2 cm, width = 2 cm, thickness = 0.08 cm). The coupons were weighed by an analytical balance, with a precision of 0.1 mg, before the tests. After the immersion, the coupons were taken out from the solution, and then they were washed with a bristle brush under running water, degreased in acetone, rinsed with ethanol, dried by a hot air stream and accurately re-weighed. Three measurements were performed in each case, and the mean value of the weight loss has been reported.

Electrochemical methods

Potentiodynamic polarization and electrochemical impedance spectroscopy experiments were performed using a Volta laboratory (Tacussel- Radiometer

PGZ 100) potentiostat controlled by a Tacussel corrosion analysis software model (Volta-master 4), under static conditions. The EIS data were fitted by Zview2 software. A conventional three-electrode system was used for potentiodynamic polarization and electrochemical impedance measurement. It consists of carbon steel as working electrode (1 cm^2), platinum as counter electrode and a saturated calomel electrode (SCE) as reference. Prior to each electrochemical test, an immersion time of 30 min at Open Circuit Potential (OCP) was given to allow system stabilization at corrosion potential. EIS tests, in the absence and presence of inhibitors, were performed at free potential, in the frequency range from 10 mHz to 100 kHz, with an amplitude of the voltage perturbation of 10 mV AC peak-to-peak, at OCP. Nyquist plots were made from these experiments. Charge transfer resistance (R_{ct}), double layer capacitances (C_{dl}) and other parameters were calculated by fitting Nyquist plot. The polarization measurements were carried out at the corrosion potential range from -600 to -200 mV/SCE versus OCP. The scan rate was 1 mV s^{-1} , as this value allowed the quasi-stationary state measurements. Electrochemical parameters, such as corrosion current density (i_{corr}), corrosion potential (E_{corr}), cathodic (β_c) and anodic (β_a) Tafel slopes, were derived by the extrapolation. Inhibition efficiencies were determined from corrosion currents calculated by the Tafel extrapolation method and from fitting the linear part of the curve to the polarization equation.

Quantum chemical studies

Density Functional Theory (DFT) was performed to explore the relationship between inhibitors molecular properties and inhibition efficiency. More accurately, DFT gives insights on the electronic and adsorption properties of some inhibitors active constituents. DFT calculations for benzimidazole derivatives were carried out with the Lee–Yang–Parr nonlocal correlation functional (B3LYP) and 6-31G (d, p) basis set implemented in Gaussian 09 program package¹⁸. In order to understand the reactivity of these compounds, several theoretical parameters, such as the energies of the highest occupied and lowest unoccupied molecular orbitals (E_{HOMO} and E_{LUMO}), energy gap (ΔE), dipole moment (μ), global hardness (η), softness (σ) and fraction of electrons transferred from the inhibitor molecule to the metal surface (ΔN), were determined and discussed.

On the other hand, interaction energies between the studied benzimidazole derivatives and the Fe(110) surface have been evaluated by MD simulation technique, using Materials Studio 7.0 (from Accelrys Inc.). The interaction of the inhibitor molecules with the metallic surface was modeled based on the adsorption of a single inhibitor molecule on the Fe(110) crystal surface. After constructing the initial geometry of the surface and of the inhibitor molecules, geometry optimization was done, in order to get rid of the unfavorable structures and minimize the energy of the initial geometries. The structure of the inhibitor molecule was first optimized using the Condensed-phase Optimized Molecular Potentials for Atomistic Simulation Studies (COMPASS) force field. Fe crystal was cleaved into a 110 plane to obtain a Fe(110) crystal plane. COMPASS force

field was then used to optimize the surface to a minimum energy. The optimized Fe(110) was enlarged to a 10x10 supercell, and a vacuum slab of zero thickness was built above the plane. A supercell, with a size of $a = b = 24.82 \text{ \AA}$ $c = 25.14 \text{ \AA}$, containing 500 H_2O , 9Cl^- , $9\text{H}_3\text{O}^+$ and a molecule of tested benzimidazole derivatives, was created. The MD simulations were performed under a canonical ensemble (NVT), at a temperature of 298 K, using a time step of 1.0 fs and a simulation time of 500 ps. The adsorption strengths between the inhibitor species and Fe (110) were evaluated by calculating the interaction energies, using the following equations¹⁹:

$$E_{\text{interaction}} = E_{\text{total}} - (E_{\text{surface+solution}} + E_{\text{inhibitor}}) \quad (1)$$

$$E_{\text{Binding}} = -E_{\text{interaction}} \quad (2)$$

where E_{total} is the total energy of the entire system, $E_{\text{surface+solution}}$ is the energy of the iron surface and the solution without the inhibitor and $E_{\text{inhibitor}}$ represents the total energy of the inhibitor.

Results and discussion

Effect of inhibitor concentration

Weight loss study

Carbon steel corrosion in a 1 M HCl solution, containing various concentrations of EMSB, MSVB and MSBP, after 6 h of immersion, at 303 K, was evaluated using weight loss technique. The corrosion rate, (W), inhibition efficiency, $\eta_{\text{WL}}(\%)$, and surface coverage obtained for carbon steel are listed in Table 2. The following equations were used to calculate the inhibition efficiency and the surface coverage (θ):

$$\eta_{\text{WL}}(\%) = \left[\frac{W^\circ - W}{W^\circ} \right] \times 100 \quad (3)$$

$$\theta = \left[\frac{W^\circ - W}{W^\circ} \right] \quad (4)$$

where W and W° are the carbon steel corrosion rates with and without inhibitors, respectively and θ is the degree of the inhibitors surface coverage.

Fig. 1a illustrates the influence of the increased inhibitors concentrations tested on CS corrosion rate in a 1 M HCl solution. It is obvious that the corrosion rate decreases with higher inhibitor concentrations, which suggests the retardation of CS corrosion, in the presence of benzimidazole derivatives, with respect to the plain acid (1 M HCl). The variation in inhibition efficiency of benzimidazole derivatives with their concentrations is shown in Fig. 1b. It seems from this figure that the inhibition efficiency, $\eta_{\text{WL}}(\%)$, of the inhibitors increases with higher concentrations, reaching a maximum values at 10^{-3} M . It is further evident that all three inhibitors showed appreciably high $\eta_{\text{WL}}(\%)$, even at a concentration as low as 10^{-6} M . The $\eta_{\text{WL}}(\%)$, for EMSB, MSVB and MSBP, was found to be 90, 93

and 94%, respectively, at 10^{-3} M, and 68, 79, 85%, at 10^{-6} M, respectively (Table 2). The increase in $\eta_{WL}(\%)$ with higher inhibitors concentrations was due to an increase in the surface coverage, which resulted in an enhanced retardation of metal dissolution in the aggressive media²⁰. MSBP, with three N, one S and four O-atoms in its molecular structure, showed better inhibition performance than EMSB and MSVB. This further supports previous reports that the presence of heteroatoms in an organic molecule facilitates the adsorption onto the metal surface and, therefore, enhances corrosion inhibition efficiency²¹⁻²³.

Table 2. Corrosion rate and inhibition efficiency for CS corrosion in 1 M HCl, with and without various concentrations of benzimidazole derivates, at 303 K.

Inhibitors	Concentration (M)	W (mg/cm ² × h)	η_{WL} (%)	θ
Blank	1	1.135	-	-
EMSB	1×10^{-6}	0.363	68	0.68
	1×10^{-5}	0.249	78	0.78
	1×10^{-4}	0.181	84	0.84
	1×10^{-3}	0.113	90	0.90
MSVB	1×10^{-6}	0.238	79	0.79
	1×10^{-5}	0.192	83	0.83
	1×10^{-4}	0.102	91	0.91
	1×10^{-3}	0.079	93	0.93
MSBP	1×10^{-6}	0.170	85	0.85
	1×10^{-5}	0.124	89	0.89
	1×10^{-4}	0.091	92	0.92
	1×10^{-3}	0.068	94	0.94

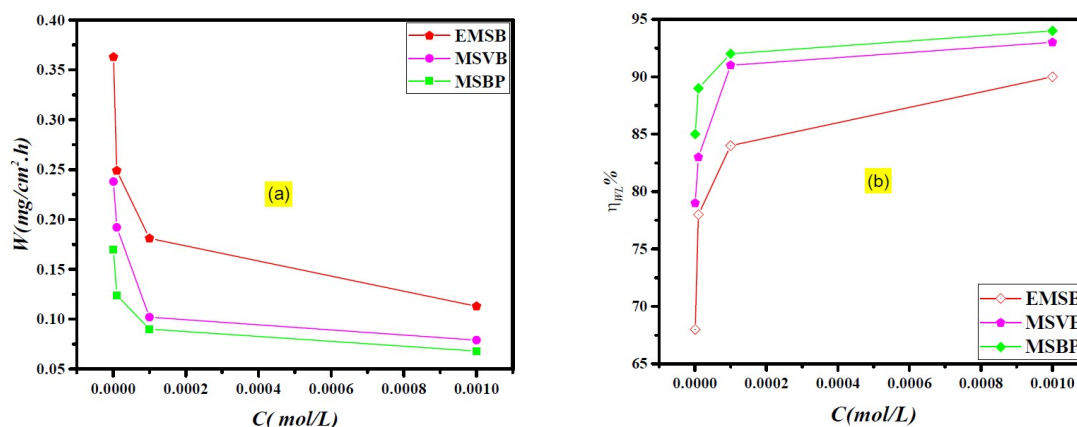


Figure 1. Variation of (a) W and (b) $\eta_{WL}(\%)$ with the concentrations of benzimidazole derivates in a 1 M hydrochloric acid solution.

Potentiodynamic polarization curves

Polarization is an opposite measurement for identifying the effect of an inhibitor on both anodic and cathodic reactions. Potentiodynamic polarization curves of CS in 1 M HCl, without and with different concentrations of benzimidazole derivates, at 303 K, are given in Fig. 2. The electrochemical parameters were obtained by extrapolating the anodic and cathodic Tafel regions of the curves to

the point of intersection with E_{corr} . The corrosion inhibition efficiency, $\eta_{\text{PDP}}(\%)$, was calculated using the relation (5):

$$\eta_{\text{PDP}}(\%) = \left[1 - \frac{i_{\text{corr}}}{i_{\text{corr}}^0} \right] \times 100 \quad (5)$$

where i_{corr} and i_{corr}^0 are the corrosion current density in inhibited and uninhibited acids, respectively. The values of i_{corr} , E_{corr} , $\eta_{\text{PDP}}(\%)$, cathodic and anodic Tafel line, as a function of inhibitors concentrations, are given in Table 3.

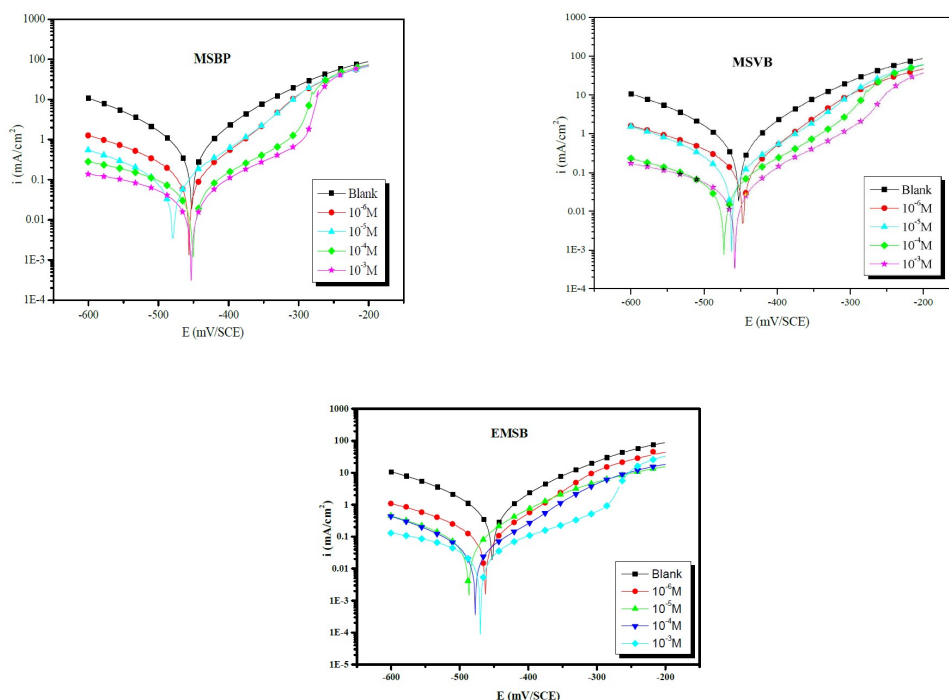


Figure 2. Potentiodynamic polarization curves for carbon steel in 1 M HCl, without and with different concentrations of EMSB, MSVB and MSBP.

The polarization curves in Fig. 2 show that the addition of these organic compounds to the corrosive medium (1 M HCl) leads to a decrease in the corrosion currents densities for both cathodic and anodic reactions. This effect is all the more noticeable when the concentration of added compounds increases. These results suggest that benzimidazole inhibitors reduce anodic dissolution and delay the reduction of H^+ protons.

On the other hand, anodic Tafel curves reveal that the inhibition process of the studied benzimidazole derivatives depends on the electrode potential^{24,25}. In fact, the anodic domain of these inhibited polarization curves shows an irregularity in their shape, particularly around -250 mV (desorption potential). In other words, when the potentials became more positive than the desorption potential, i.e., -250 mV, there was little effect on the presence of the benzimidazole compounds, implying that carbon steel dissolution is more dominant than the inhibitor molecules adsorption. So, it can be noted that the inhibitor molecules (even at high concentrations) adsorbed onto the steel surface begin to disappear, and no longer can sufficiently protect carbon steel at a higher potential than

desorption potential. This can be attributed to an increase in the surface area, as carbon steel is dissolving, and, simultaneously, as benzimidazole inhibitors are being adsorbed onto the metal surface; so, the adsorption rate of the benzimidazole derivatives is lower than their desorption rate. This finding is consistent with other research which found that an increase in anodic currents is mainly associated with the desorption potential that alters significantly the inhibitor film²⁶. In addition, the polarization curves showed a slight shift of the corrosion potential to more negative values. An inhibitor may be classified as of the cathodic or anodic type, if the displacement in corrosion potential is greater than 85 mV, with respect to the corrosion potential of the control solution²⁷. In our study, the maximum displacement was lower than 85 mV/ E_{corr} , which indicates that the organic compounds acted as mixed-type inhibitors.

Table 3. Electrochemical parameters for carbon steel in 1 M HCl, at various concentrations of EMSB, MSVB and MSBP, at 303 K.

Inhibitors	Concentration (M)	$-E_{\text{corr}}$ (mV/SCE)	i_{corr} ($\mu\text{A cm}^{-2}$)	β_a (mV dec ⁻¹)	$-\beta_c$ (mV dec ⁻¹)	η_{PDP} (%)	θ
HCl	1.0	452	507	100	122	-	-
EMSB	1×10^{-6}	465.1	126.5	84.5	148.6	75	0.75
	1×10^{-5}	489.6	101.0	103.5	176.7	80	0.80
	1×10^{-4}	480.1	52.1	93.3	139.3	89	0.89
	1×10^{-3}	472.4	40.2	159	161	92	0.29
MSVB	1×10^{-6}	446	96	71	100	81	0.81
	1×10^{-5}	462	71	84	87	86	0.86
	1×10^{-4}	473	35	92	133	93	0.93
	1×10^{-3}	457	25	81	135	95	0.95
MSBP	1×10^{-6}	455	51	62	74	90	0.90
	1×10^{-5}	479	36	78	89	93	0.93
	1×10^{-4}	451	20	61	75	96	0.96
	1×10^{-3}	453	15	65	97	97	0.97

Furthermore, in the cathodic domain, the addition of the inhibitors to a corrosive medium results in a significant decrease in the cathodic partial current, as well as in a slight modification of the cathode Tafel slopes. These branches have a wide range of linearity, which proves that Tafel's law is well verified in this domain. These notes show that the reduction of H^+ protons on the carbon steel surface is not modified by the inhibitors addition, and that it is carried out according to a pure activation mechanism. The inhibitor appears to be adsorbed first onto the metal surface, before acting by simple blocking the active sites²⁸. From the results presented in Table 3, it can be seen that i_{corr} values determined by extrapolation of the cathodic lines decrease as the inhibitors concentration increases, and that $\eta_{\text{PDP}}(\%)$ values increase with higher concentrations, reaching a maximum of 92 %, 95%, and 97%, respectively, at 10^{-3} M, for EMSB, MSVB, and MSBP. The observed trend manifests that the phenacyl substituted MSBP derivative has better blocking ability than that of the alkyl chains substituted

derivatives. The potentiodynamic data confirm the conclusions of the gravimetric tests, giving some additional information about the inhibition type.

Electrochemical Impedance Spectroscopy (EIS)

Electrochemical impedance spectroscopy (EIS) allows the study of the resistive and capacitive behavior at the interface and the evaluation of the performance of the compounds tested as metallic corrosion inhibitors. Fig. 3 provides Nyquist plots for carbon steel in a 1 M HCl solution, without and with different concentrations of EMSB, MSVB and MSBP.

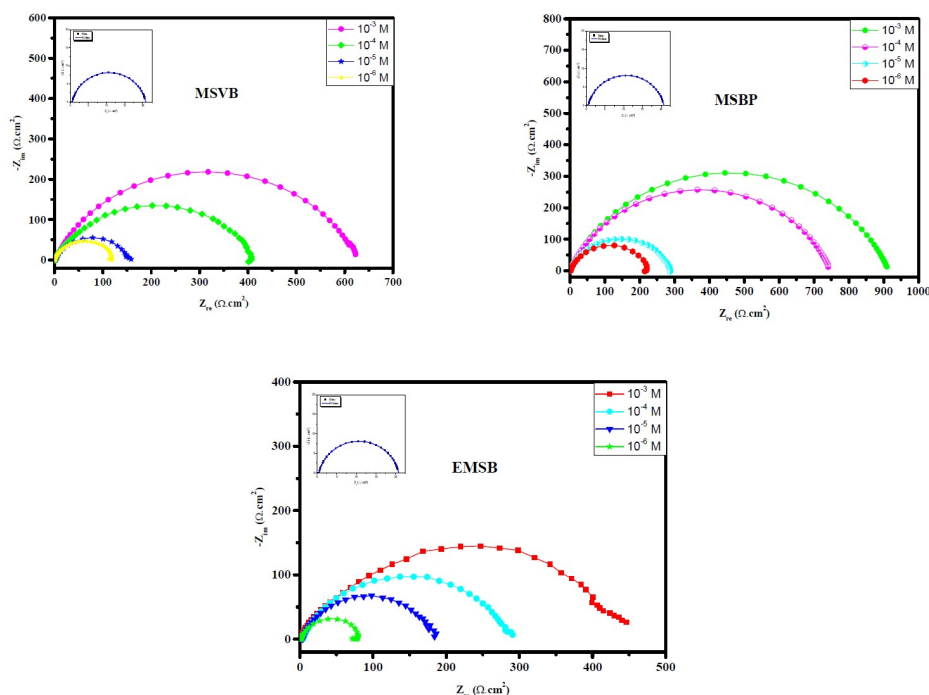


Figure 3. Nyquist plots for carbon steel in a 1.0 M HCl solution, in the absence and presence of various concentrations of benzimidazole derivatives.

This figure shows that the impedance patterns have the shape of a depressed semicircle. It is clear from this figure that the impedance response of CS (diameter of the semicircle) has changed considerably after the inhibitors addition to the corrosive solution. Though the curves are in a depressed form, the diameter of the semicircle increased at each higher concentration level, which is related to a decrease in active sites. This suggests that the metal surface was protected from the acidic environment, and that maximum protection was attained at optimum concentrations, which afforded highest inhibition efficiency. It should be noted that the modification of EMSB, MSVB and MSBP concentrations did not alter the shape of the impedance behavior, suggesting a similar mechanism for carbon steel corrosion inhibition. High resistance to charge transfer is associated with a slow corrosion system.

CPE could be treated as a parallel combination of a pure capacitor with a resistor, being inversely proportional to the angular frequency and its impedance (Fig. 4), which are given by:

$$Z_{CPE} = \frac{1}{Q(j\omega)^n} \quad (6)$$

where Q is the CPE magnitude (in $\Omega^{-1} \times \text{Sn} \times \text{cm}^{-2}$), j is the imaginary unit, ω is the angular frequency (in rad s^{-1} ; $\omega = 2\pi f$, where f is the AC frequency) and n is the exponential term of a CPE that can be used as a measure of surface inhomogeneity. To obtain a direct correlation between charge-transfer resistance (R_{ct}) and double layer capacitance (C_{dl}), the later has been recalculated using the following equation³⁰:

$$C_{dl} = \sqrt[n]{Q \times R_{ct}^{1-n}} \quad (7)$$

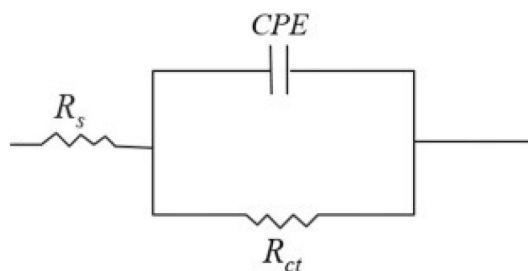


Figure 4. Equivalent circuit used to model impedance data.

The percentage inhibition efficiencies, $\eta_{R_{ct}}$, in terms of R_{ct} , are calculated through the following equation:

$$\eta_{R_{ct}} (\%) = \left[\frac{R_{ct(inh)} - R_{ct}}{R_{ct(inh)}} \right] \times 100 \quad (8)$$

where $R_{ct(inh)}$ and R_{ct} are the charge transfer resistance values, with and without inhibitor, respectively. The value of double layer capacitance (C_{dl}) and the inhibitory efficiency are also listed in Table 4.

It is apparent from the parameters of this table that the impedance of the inhibited system is amplified with increased inhibitor concentrations, and that R_{ct} values, in the inhibitors presence, are higher than those of R_{ct} for the blank. The increase in R_{ct} values is attributed to the formation of an insulating protective film of the inhibitors at the metal/solution interface. CPE value decreases with higher concentrations of all the three inhibitors, indicating the adsorption of the inhibitor molecules onto the carbon steel surface. R_{ct} values increase with higher concentrations, while C_{dl} values generally decrease. C_{dl} decrease is associated to the increase in thickness of the electrical double layer, as a result of the inhibitor adsorption onto carbon steel^{31,32}. Also, it is the manifestation of the removal of water molecules and of other pre-adsorbed ions (here, chloride) from the metal surface by the inhibitor molecules³⁰. It is clear that there is a causal relationship between adsorption and inhibition. In addition, it is evident that the inhibitory efficiency increases with higher inhibitor concentrations. From the table, adsorption capacity and, hence, the inhibitive performance, were observed to vary in the order MSBP > MSVB > EMSB. Furthermore, Table 4 shows that the

corrosion inhibition efficiency obtained from EIS measurements is consistent with that obtained from PDP and from weight loss methods.

Table 4. Electrochemical impedance parameters for carbon steel in a 1.0 M HCl solution, without and with different concentrations of benzimidazole derivatives, at 303 K.

Medium	Concentration (M)	R_s ($\Omega \text{ cm}^2$)	R_{ct} ($\Omega \text{ cm}^2$)	$Q \times 10^{-4}$ ($\Omega^{-1} \text{ cm}^2 \text{ s}^n$)	n	C_{dl} ($\mu\text{F cm}^{-2}$)	η_{Rct} (%)
Blank	1,0	0,568	20,24	2.420	0.860	112.04	-
EMSB	1×10^{-6}	0.961	67.2	1.430	0.81	48.09	69
	1×10^{-5}	1.826	126.0	0.762	0.85	33.56	83
	1×10^{-4}	1.840	202.0	0.930	0.75	26.72	89
	1×10^{-3}	0.760	335.0	0.567	0.81	22.37	93
MSVB	1×10^{-6}	1.247	119.2	1.020	0.82	41.09	83
	1×10^{-5}	1.407	150.7	0.942	0.80	32.97	87
	1×10^{-4}	1.062	406.4	0.810	0.74	25.39	95
	1×10^{-3}	1.067	621.2	0.563	0.78	21.99	97
MSBP	1×10^{-6}	1.309	221.1	0.830	0.80	31.32	91
	1×10^{-5}	1.215	283.5	0.780	0.79	29.54	93
	1×10^{-4}	1.012	738.7	0.501	0.78	20.11	97
	1×10^{-3}	1.047	913.5	0.479	0.78	19.93	98

Temperature effect

The temperature effect on carbon steel corrosion behavior in an acidic solution (1 M HCl), in the absence and the presence of 10^{-3} M of inhibitors, was studied in the temperature range from – 303 to 333K, using PDP measurements. The potentiodynamic polarization curves are represented in Figs. 5 and 6.

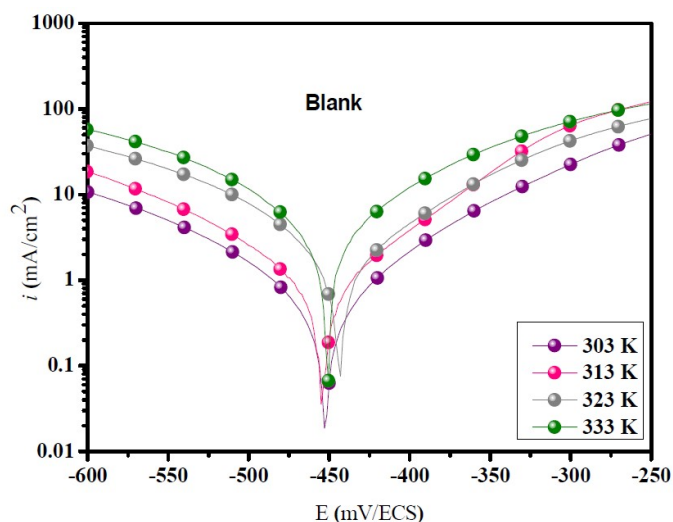


Figure 5. Potentiodynamic polarization curves for carbon steel in 1.0 M HCl, without inhibitors, at different temperatures.

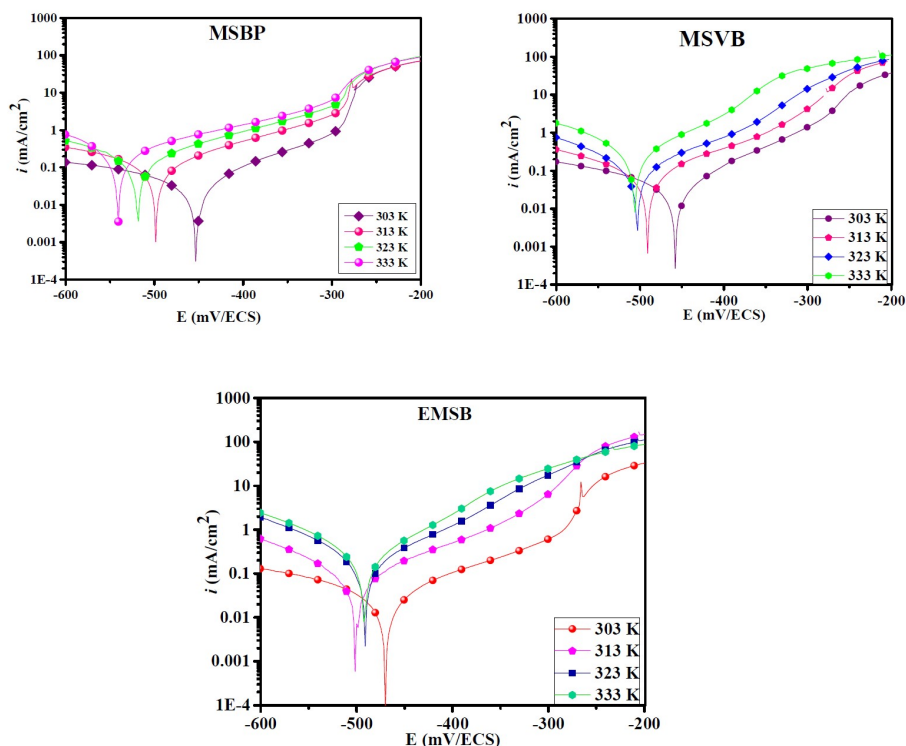


Figure 6. Potentiodynamic polarization curves for carbon steel in 1.0 M HCl, in the presence of 1×10^{-3} M of benzimidazole derivatives, at different temperatures.

Table 5. Corrosion parameters obtained from PDP measurements of carbon steel in a 1 M HCl solution, in the presence and absence of 1×10^{-3} M of inhibitors, at different temperatures.

Medium	T	E_{corr}	i_{corr}	η_{PDP}	θ
Blank	303	-452	507	-	-
	313	-454	860	-	-
	323	-443	1840	-	-
	333	-450	2800	-	-
MSVB	313	-503	91	89	0.89
	323	-493	251	86	0.86
	333	-494	616	78	0.78
	303	-457	26	95	0.95
MSBP	313	-490	65	92	0.92
	323	-503	175	90	0.90
	333	-505	361	87	0.87
	303	-453	16	97	0.97
EMSB	313	-497	57	93	0.93
	323	-518	150	92	0.92
	333	-541	283	90	0.90
	303	-453	16	97	0.97

Table 5 regroups the obtained corresponding results. From the experimental data (Table 5), we note that the corrosion current density increases both in the uninhibited and inhibited acidic solution, with a temperature rise. We also noticed that carbon steel corrosion rate, in the inhibitors absence, increased steeply from 303 to 333K, whereas it increased slowly in the inhibitors presence. It is also clear from Table 5 that $\eta_{PDP}\%$ decreased with higher temperatures, from 303 to 333 K. These results can be described on the basis that an increase in

temperature leads to a shift of the equilibrium position of the adsorption/desorption phenomena towards the desorption of the inhibitors molecules at the carbon steel surface³³.

Additionally, the effect of temperature on the nature of carbon steel dissolution in 1 M HCl can be best explained in terms of Arrhenius equation. The apparent activation energy (E_a) for carbon steel dissolution in a 1 M HCl solution, without and with various inhibitors concentrations, was calculated by using Arrhenius equation (9):

$$i_{corr} = K \exp\left(\frac{-E_a}{RT}\right) \quad (9)$$

where E_a is the apparent activation energy, R is the molar gas constant ($8.314 \text{ J K}^{-1} \text{ mol}^{-1}$), T is the absolute temperature and K is the Arrhenius pre-exponential factor. The Arrhenius plots of $\ln(i_{corr})$ against $1/T$, for carbon steel corrosion in a 1 M HCl solution, in the absence and presence of various concentrations of EMSB, MSVB and MSBP, are shown in Fig. 7. The slopes of the lines were determined, and the respective E_a values were calculated from the slopes of the plots, as shown in Fig. 7. The calculated E_a values are listed in Table 6. It is obvious that the inhibitors presence (dosage of 10^{-3} M) in acidic media increases the activation energy (E_a), compared to the blank value. This result indicates that carbon steel dissolution becomes difficult in the studied inhibitors presence. This is due to an increase in the energy barrier for the dissolution reaction, which in turn is associated with the inhibitors adsorption onto the metal surface³⁴.

The thermodynamic parameters (enthalpy, ΔH_a , and entropy, ΔS_a , of activation) for carbon steel corrosion in a free 1 M HCl solution, and in that containing 10^{-3} M of inhibitors in 1 M HCl, were calculated from the slopes and intercepts of lines in Fig. 8, using the following equation:

$$i_{corr} = \left(\frac{RT}{Nh}\right) \exp\left(\frac{\Delta S_a}{R}\right) \exp\left(\frac{-\Delta H_a}{RT}\right) \quad (10)$$

where N is the Avogadro number and h is Planck constant.

A plot of $\ln \frac{i_{corr}}{T}$ against $\frac{1}{T}$ (Fig. 8) gave straight lines with a slope of $\frac{-\Delta H_a}{R}$ and an intercept of $\ln \frac{R}{Nh} + \frac{\Delta S_a}{R}$, from which the value of activation thermodynamic parameters, such as ΔH_a and ΔS_a , was calculated and is listed in Table 6. The higher ΔH_a value indicates the creation of an energy barrier for the corrosion reaction in the inhibitor presence. ΔH_a positive values reflect the endothermic nature of the dissolution of the tested alloy in the corrosive media. ΔS_a negative values for the three inhibitors indicate that the formation of the activated complex in the rate determining step represents an association rather than a dissociation step, meaning that a decrease in disorder lines takes place during the course of the transition from reactants to the activated complex³⁵. Table 6 reveals that E_a and ΔH_a values have a similar trend variation, thus proving the well-

known thermodynamic formula (6), which further confirms and validates all these interpretations:

$$E_a - \Delta H_a \approx R \times T \quad (11)$$

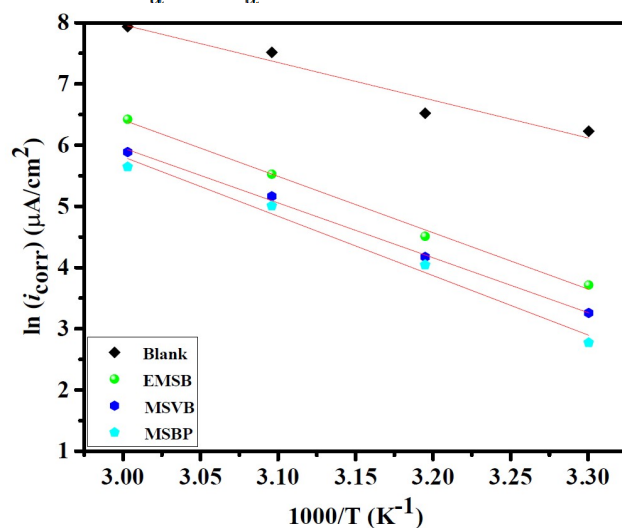


Figure 7. Arrhenius plots for C-steel, in the absence and presence of 10^{-3} M of inhibitors.

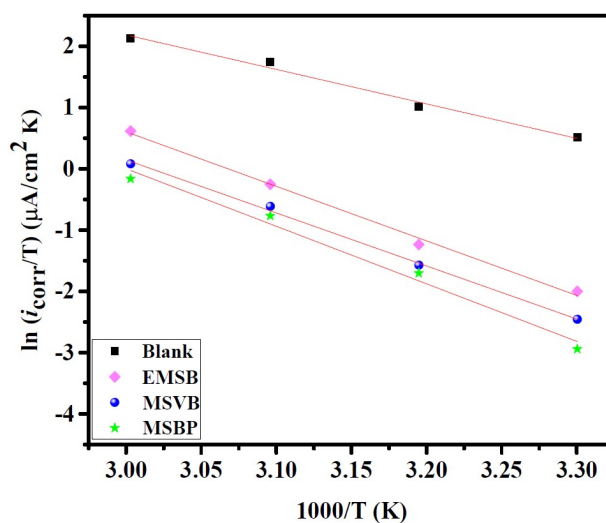


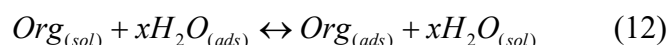
Figure 8. Alternative Arrhenius plots for C-steel, in the absence and presence of 10^{-3} M of inhibitors.

Table 6. Activation parameters for the dissolution of C-steel in 1 M HCl, with and without 10^{-3} M of benzimidazole derivatives.

Inhibitor	E_a (kJ mol ⁻¹)	ΔH_a (kJ mol ⁻¹)	ΔS_a (J mol ⁻¹ K ⁻¹)	$E_a - \Delta H_a$
Blank	49.38	46.77	-38.96	4.48
MSBP	80.70	78.06	36.74	2.64
MSVB	74.56	71.93	19.54	2.63
EMSB	76.60	73.96	29.45	2.64

Adsorption isotherm

In order to give basic information about the adsorption interaction occurred in the investigated corrosive medium, the adsorption isotherm was studied. The adsorption process is affected by several factors, such as the type of corrosive environment, the chemical structure of an organic inhibitor, the distribution of charge in the molecule and the nature properties of the metal surface, etc. The adsorption of organic molecules from the aqueous solution can be regarded as a quasi-substitution process between the organic compound in the aqueous phase [org(sol)] and water molecules at the electrode surface [$H_2O_{(ads)}$]³⁶:



where x is the number of water molecules replaced by one organic inhibitor and $Org_{(sol)}$ and $Org_{(ads)}$ are the organic molecule in the solution and the molecule adsorbed onto the steel surface, respectively. In order to find the best adsorption isotherm, which characterizes the adsorption of the investigated benzimidazole inhibitors onto the carbon steel surface, different isotherm types were employed to fit the empirical data, such as Langmuir, Frumkin and Temkin models. In this study, the adsorption mechanism was determined by fitting the θ values obtained from potentiodynamic polarization data, to obtain the best adsorption isotherm at various concentrations. The experimental data were fitted into various adsorption isotherms, but Langmuir isotherm gave the best linear plots. The Langmuir isotherm is described according to the following equation:

$$\frac{C_{inh}}{\theta} = \frac{1}{K_{ads}} + C_{inh} \quad (13)$$

where K_{ads} is the equilibrium constant for the adsorption–desorption process, C_{inh} is the inhibitor molar concentration in the solution and θ is the degree of surface coverage. The plots of C_{inh}/θ vs C_{inh} yielded straight lines, as shown in Fig. 9. The slope and the correlation coefficient (R^2) values for the Langmuir adsorption plots are listed in Table 7. It is seen that Langmuir adsorption plots (Fig. 9) of the inhibitors gave straight lines with an excellent correlation coefficient (R^2). The results suggest that the adsorptions of benzimidazole inhibitors onto the steel surface obeyed to a Langmuir adsorption isotherm. From Table 7, it can be seen that K_{ads} values for all the three studied inhibitors are relatively high, reflecting the high adsorption ability of these inhibitors onto the carbon steel surface³⁷. The interaction can be associated to lone pairs of electrons of N, O and S atoms, π -electrons, for each of the studied compounds, and to the vacant d-orbitals of iron surface atoms. Using K_{ads} values, the ΔG_{ads} values were calculated by the following equation:

$$\Delta G_{ads} = -RT \ln(K_{ads} \times 55.5) \quad (14)$$

where T is the absolute temperature, R is the gas constant and 55.5 is the molar concentration of water.

It can also be seen from Table 7 that the obtained ΔG_{ads} values are negative. The negative value of adsorption-free energy suggests the spontaneity of the adsorption of benzimidazole molecules and the stability of the adsorbed layer onto the carbon steel surface³⁸. In general, ΔG_{ads} values up to -20 kJ mol^{-1} are associated with the electrostatic interaction between the charged inhibitor molecules and the charged metal surface (physisorption); whereas, when ΔG_{ads} is -40 kJ mol^{-1} or lower, it involves the sharing or charge transfer from the inhibitor molecules to the metal surface (chemisorption)³⁹. In the present study, ΔG_{ads} values for EMSB, MSVB and MSBP are between -43.7 and -46.5 , indicating that the adsorption of the studied inhibitors onto the metallic surface mostly obeyed to the chemisorption mechanism.

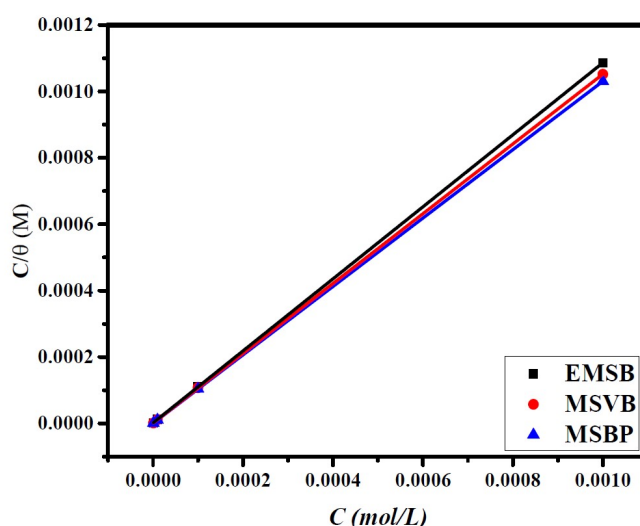


Figure 9. Langmuir adsorption plots for the adsorption of MSBP, MSVB and EMSB onto the carbon steel surface, in 1 M HCl.

Table 7. Thermodynamic parameters for the adsorption of MSBP, MSVB and EMSB estimated from Langmuir adsorption isotherm, for carbon steel, at 303 K.

Inhibitors	R^2	$K_{\text{ads}}(\text{M}^{-1})$	$\Delta G_{\text{ads}}(\text{kJ/mol})$
MSBP	1.00	1939600	-46.5
MSVB	1.00	851571	-44.1
EMSB	1.01	633793	-43.7

Computational studies

DFT calculations

In order to afford insights on the structural and electronic properties of the various active sites of benzimidazole derivatives, DFT calculations were particularly employed, since the molecular structure is one of the major factors influencing the organic molecules adsorption onto the metal surface and, hence, the inhibitor properties, especially in the case of chemisorption, which involves charge sharing or charge transfer from the inhibitor molecules to the metal, to

form the coordinate type of bonds. Through geometrical optimization and investigation of frontier molecular orbitals (FMO), highest occupied molecular orbital (HOMO) and lowest unoccupied molecular orbital (LUMO), one can predict the nature, as well as the extent of the inhibitor molecules adsorption^{40,41}. The adsorption of organic compounds onto the metallic surface occurs principally through donor-acceptor interaction. It is generally assumed that the electron donating ability of a molecule increases with higher E_{HOMO} values, whereas a lower E_{LUMO} value indicates the molecule to be more susceptible towards accepting electrons^{42,43}. Fig. 10 presents the optimized structures, HOMO and LUMO electron density of the studied molecules. The calculated quantum chemical parameters, such as E_{HOMO} , E_{LUMO} , ΔE , and ΔN , are represented in Table 8. The ionization potential (IP) and electron affinity (EA) were deduced from E_{HOMO} and E_{LUMO} , using Eqs. (15) and (16):

$$IP = -E_{\text{HOMO}} \quad (15)$$

$$EA = -E_{\text{LUMO}} \quad (16)$$

Meanwhile, electronegativity (χ) and chemical hardness (η) were evaluated based on the finite difference approximation, using the following relations^{44,45}:

$$\chi = \frac{IP + EA}{2} \quad (17)$$

$$\eta = \frac{IP - EA}{2} \quad (18)$$

Kokalj recently reported⁴⁶ that the work function (ϕ) of a metal surface is an appropriate measure of its electronegativity, and should be used together with its vanishing absolute hardness, to estimate the fraction of transferred electrons (ΔN), using the equation:

$$\Delta N = \frac{\phi - \chi_{\text{inh}}}{2(\eta_{\text{Fe}} + \eta_{\text{inh}})} \quad (19)$$

where (ϕ) and χ_{inh} denote the work function and absolute electronegativity of iron and the inhibitor molecule, respectively and η_{Fe} and η_{inh} denote the absolute hardness of iron and the inhibitor molecule, respectively. The theoretical values of χ_{Fe} and η_{Fe} are 7 and 0, respectively. They were considered in order to calculate the ΔN values. A theoretical value for the work function ($\phi = 4.82$ eV) of Fe(110) plane was used^{46,47}. The molecule with the highest E_{HOMO} values indicates that it has a high tendency to donate electrons to appropriate acceptor molecules with low energy empty molecular orbitals. The lower E_{LUMO} value for a molecule suggests that it can readily accept electrons from the donor molecules⁴⁸. As a result, the molecule with the lower absolute value of the energy band gap ($\Delta E = E_{\text{LUMO}} - E_{\text{HOMO}}$) exhibits higher inhibition efficiencies, because

of the possibility of both ways of electron transfer, i.e., inhibitor to metal and vice versa^{49,50}.

Upon inspection of the results, we noticed that the reactivity of the selected organic constituents would likely depend on their molecular structure. For all the three benzimidazole derivatives, the HOMO and LUMO orbitals are π -type orbitals and the electron densities are essentially delocalized over the benzimidazole ring, the adjacent pyridin group and phenacyl group, in the case of MSBP molecule. E_{HOMO} is seen to increase, at the order EMSB < MSVB < MSBP, demonstrating an enhanced ability of the inhibitor molecules to interact with the metal surface through electron donation (HOMO of the inhibitors to vacant d- orbital of Fe). E_{LUMO} follows the reverse order. This manifests that the electron accepting ability (from filled 4 s orbital of Fe to LUMO of the inhibitors) increases following the order EMSB < MSVB < MSBP. In addition, the energy band gap (ΔE) reflects the reactivity of the inhibitor molecule towards the adsorption onto the metal surface⁵¹. If ΔE increases, the reactivity of the molecule decreases, which may retard adsorption and decrease the inhibition efficiency. In Table 8, we can see that MSBP has a lower ΔE value, which suggests that this inhibitor has more potency to get adsorbed onto the carbon steel surface, resulting in a greater inhibition tendency than that of MSVB and EMSB. The reason for this is likely related to the presence of more important reactive centers in MSBP inhibitor (presence of additional heteroatoms like O, heterocyclic ring and double bonds in a conjugated system). These outcomes are in good accordance with the result obtained from experimental studies. Furthermore, ΔN value is another important index that measures the ability of a chemical compound to transfer electrons. Electron transfer will occur from the inhibitor molecule to the metal surface, if $\Delta N > 0$, and vice versa, if $\Delta N < 0$ ^{52,53}. According to Elnga et al.⁵⁴, the inhibition efficiency increases with higher electron-donating ability of the molecule at the metal surface, if $\Delta N < 3.6$. In Table 8, all ΔN values are positive and lower than 3.6, indicating that the molecules donate its electron to the Fe surface by the formation of a coordinate bond. As expected, MSBP had the highest positive ΔN values, compared to other inhibitors, which agrees well with ΔE trend. In this study, MSBP inhibition efficiency is due to the centers of adsorption on the inhibitor molecules ($=\text{N}-$, $-\text{O}-$, $=\text{O}$ and $-\text{S}=\text{O}$) and to the higher electron density caused by the electron releasing methoxy groups (OCH_3). In view of this, it is reasonable to propose that the high and stable inhibiting efficiency obtained experimentally is related to the multi-component adsorption process and/or to the synergistic effect of the multi-constituents in the benzimidazole derivatives adsorbing onto the steel surface. The graphical surfaces of the electron charge density with Mulliken charges, according to the numeration of corresponding atoms of the optimized structures of the inhibitors, are shown in Fig. 10. The general interpretation given by several authors is that the higher is the magnitude and the number of negatively charged heteroatoms present in an inhibitor molecule, the higher is its ability to be adsorbed onto the metal surface via the donor-acceptor mechanism⁵⁵.

It is clear from Fig. 11 that all three inhibitors have considerable excess of negative charge around the nitrogen atoms in the benzimidazole ring, benzene

ring, and oxygen of the methoxy group and also on some carbon atoms. This suggests that these centers are the coordinating sites through which the inhibitors will adsorb onto a positively charged metal surface.

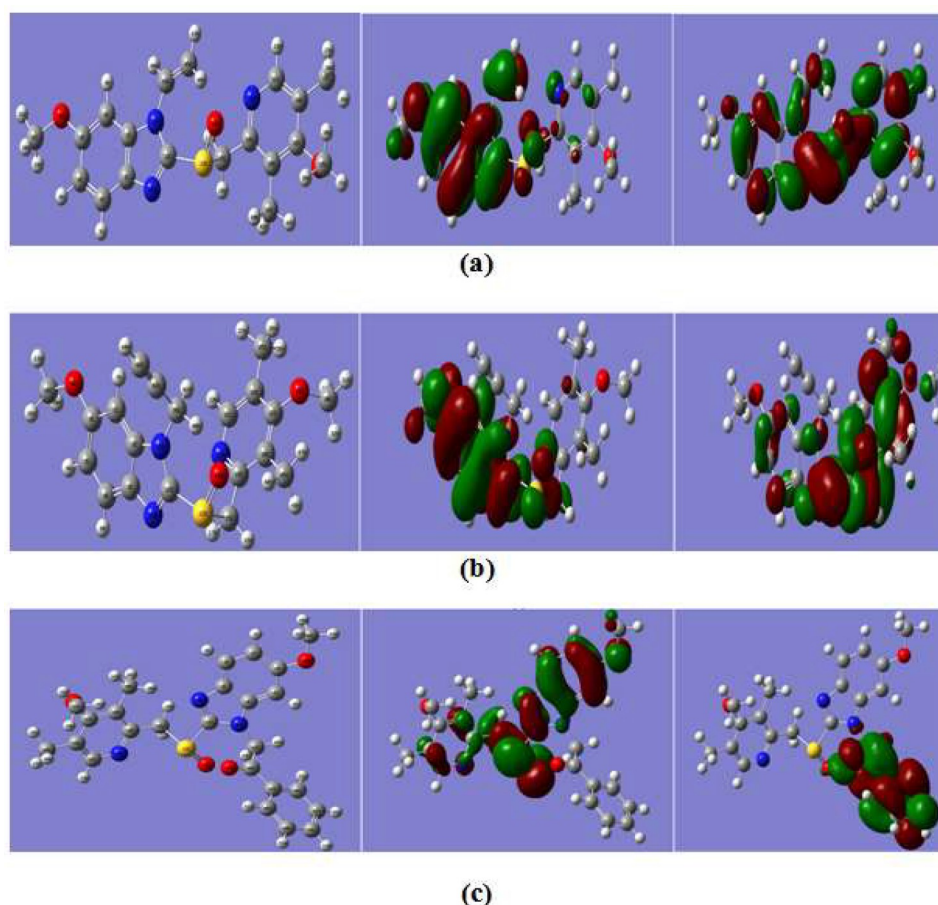


Figure 10. Optimized structure (**left**), HOMO (**center**) and LUMO (**right**) distribution for molecules (**a**) EMSB, (**b**) MSVB and (**c**) MSBP. [Atom legend: white = H; Cyan = C; blue = N; red = O].

Table 8. Calculated quantum chemical properties for the inhibitors benzimidazole derivatives obtained from DFT method.

Inhibitors	E_{HOMO}	E_{LUMO}	ΔE_{ga}	ΔN
EMSB	-5.687	-1.261	4.425	0.304
MSVB	-5.528	-1.284	4.244	0.314
MSBP	-5.501	-1.706	3.795	0.338

Molecular dynamics simulation

MD simulations are a modern tool to investigate the adsorption behavior of the inhibitor molecules on the Fe (110) surface, and, therefore, predict the adsorption ability of the inhibitors, when the adsorption process has reached equilibration. The system reaches equilibrium only if both energy and temperature are balanced. In the present study, MD simulations were used to find interaction energy for the investigated systems. The strong adsorption between the inhibitors

and the iron surface is reflected from their high negative interaction energy values.

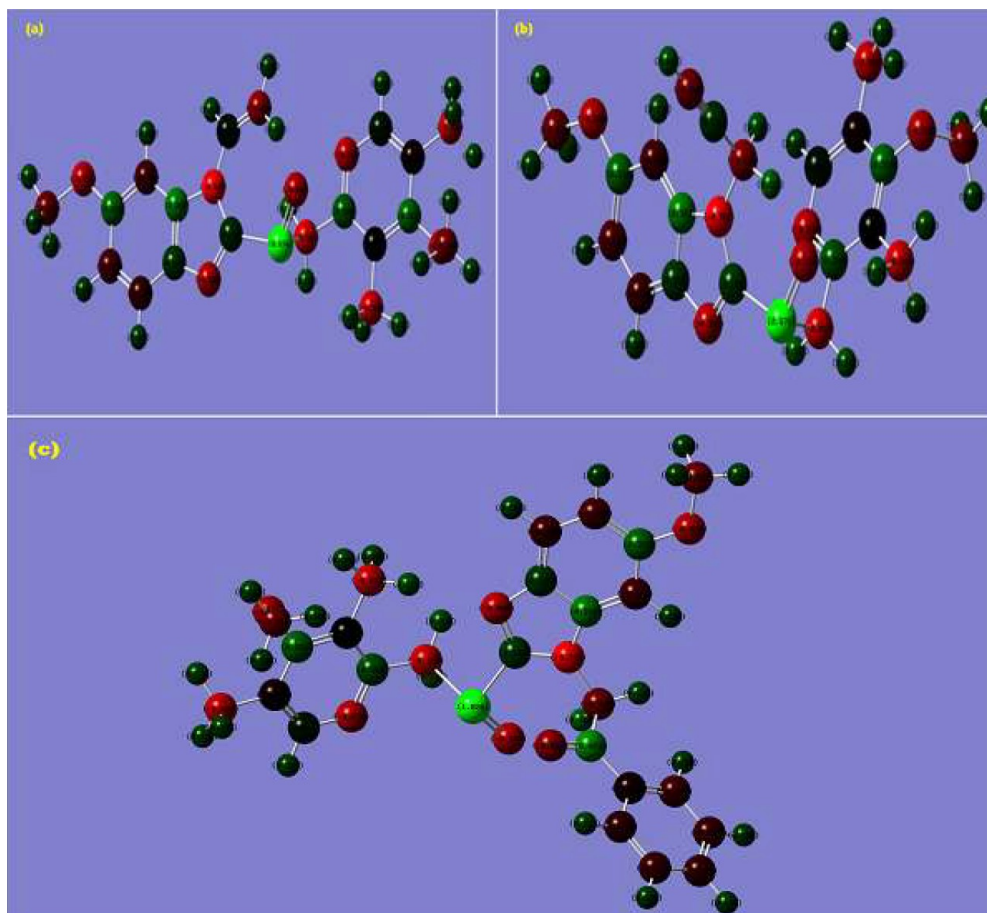


Figure 11. Mulliken charge density of (a) EMSB, (b) MSVB and (c) MSBP.

The best adsorption configurations of benzimidazole derivative on the Fe (110) surface, obtained through MD simulations, are depicted in Fig. 12. The corresponding values of the interaction energies between the inhibitor and the Fe(110) surface are listed in Table 9. As it can be seen from Fig. 12, at equilibrated state, the benzimidazole derivatives adsorb onto the Fe (1 1 0) surface, with a nearby flat orientation between the rigid structure and the metal surface. Due to the presence of unoccupied 3d-orbitals of the metal, it will prefer to accept electrons from the adsorbed inhibitor molecule. The heteroatoms and π -electrons present in benzimidazole derivatives and substituted groups ($-\text{OCH}_3$) will certainly provide sufficient electrons to the vacant metal 3d-orbitals for the formation of a stable coordination bond. On the other hand, the antibonding orbital of π -electrons in the benzimidazole and pyridine ring can also accept the electrons from 4s or 3d-orbital of iron to form feedback bonds. More interesting, the inhibitor film adsorption energies presented in Table 9 revealed very high negative values and a decrease in the order $\text{MSBP} > \text{MSVB} > \text{EMSB}$. Also, all the values of interaction energies are negative, which denotes that the adsorption could occur spontaneously^{56,57}.

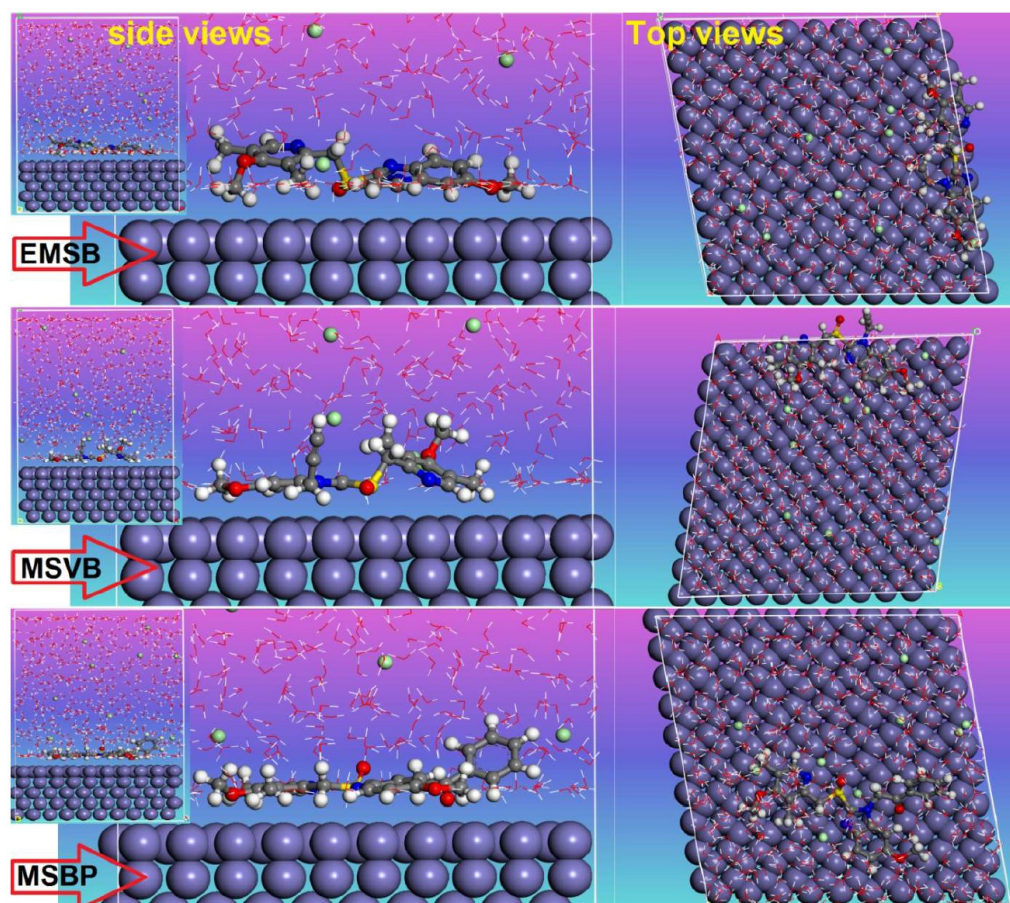


Figure 12. Side and top views of the final adsorption of the benzimidazole derivatives onto the Fe (110) surface in a solution.

Table 9. Energy parameters obtained from MD simulations for the adsorption of inhibitors on the Fe (110) surface.

System	$E_{\text{Interaction}}$	E_{Binding}
Fe + EMSb + 491H ₂ O + 9Cl ⁻ + 9 H ₃ O ⁺	-723.081	723.081
Fe + MSVB + 491 H ₂ O + 9Cl ⁻ + 9 H ₃ O ⁺	-536.104	536.104
Fe + MSBP + 491 H ₂ O + 9Cl ⁻ + 9 H ₃ O ⁺	-413.003	413.003

SEM study

Using scanning electron micrographs (SEM), the carbon steel surface is recorded, in order to evaluate the changes occurred during the corrosion process, in the absence and presence of 1×10^{-3} M of MSBP, to support our conclusion that this inhibitor is a more efficient corrosion inhibitor in the studied conditions. Fig. 13 depicts the surface photo micrographs of the steel exposed to 1 M HCl, in the absence and presence of MSBP. Considering the result of the SEM study, it can be clearly observed that the carbon steel surface, in the uninhibited solution (Fig. 12a), is seriously damaged and heterogeneous, because of the severe corrosion by the aggressive acid. This indicates a direct acid attack on the metal and a high corrosion rate without the presence of any inhibitor. However, the surface heterogeneity is considerably decreased in the presence of the MSBP inhibitor (Fig. 13b). Furthermore, the relatively smooth surface observed in the

inhibitor presence was caused by its deposition onto the carbon steel surface and, consequently, by the formation of the protective film which shields the surface against a direct acid attack.

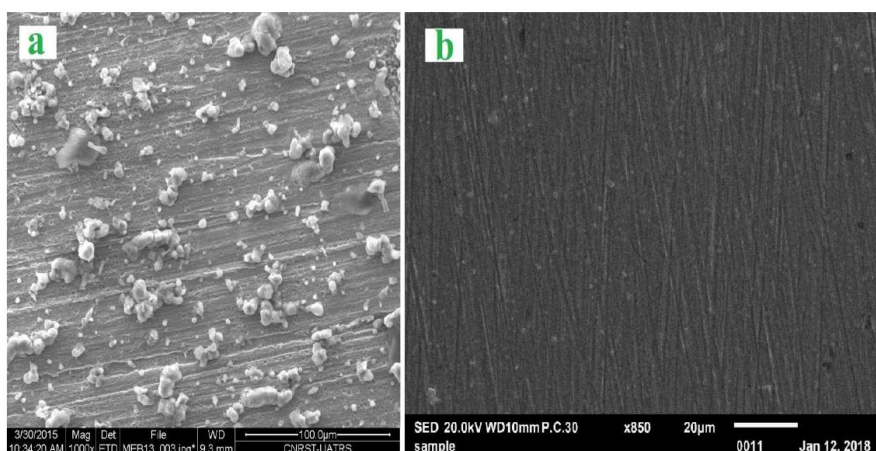


Figure 13. SEM images of the carbon steel surface after immersion for 6h in (a) 1.0 M HCl without inhibitor and (b) 1.0 M HCl + 1×10^{-3} M of MSBP.

Conclusions

This work exemplifies the effect of the nature of substituent groups on the corrosion inhibition propensity of benzimidazole derivatives towards carbon steel in 1 M HCl. Main conclusions are summarized here:

- The benzimidazole derivatives inhibitors (EMSB/MSVB/MSBP) show good inhibition efficiency for carbon steel protection in a 1 M HCl solution, and the inhibition efficiency increases with higher inhibitors concentrations and decreases with an increase in temperature. The order of the inhibition efficiency is: MSBP > MSVB > EMSB.
- Potentiodynamic polarization studies reveal the benzimidazole derivatives to have the properties corresponding to mixed type inhibitors.
- Impedance results revealed that the corrosion inhibition action was due to the adsorption of the various organic constituents of benzimidazole derivatives onto the carbon steel surface and that the adsorption process followed Langmuir adsorption isotherm.
- The thermodynamic parameters indicated that the adsorption process of the tested molecules on steel was endothermic, and the calculated ΔG_{ads} values reveal that the adsorption mechanism of EMSB, MSVB and MSBP onto the carbon steel surface was mainly chemisorption.
- The inhibitor efficiencies of these compounds seem to be determined by the conjugation of electronic factors and molecular geometry. The analysis of HOMO, LUMO and partial atomic charges suggests the centers that would be preferred for nucleophilic or electrophilic attack.
- Molecular dynamic simulations performed on the individual active constituents revealed high to reasonable adsorption strengths for most of the active species, and the high negative value of adsorption indicates the strong interaction between the metal and the investigated inhibitors.

- Planar molecular configuration, lowest energy gap between the frontier molecular orbitals, presence of pyridine and benzene ring connected with benzimidazole and other favorable molecular factors have made MSBP the most efficient corrosion inhibitor among all the three inhibitors of the present work.

References

1. Ouici HB, Benali O, Guendouzi A. Experimental and quantum chemical studies on the corrosion inhibition effect of synthesized pyrazole derivatives on mild steel in hydrochloric acid. *Res Chem Intermed.* 2016;42(9):7085–109. Doi: <https://doi.org/10.1007/s11164-016-2520-0>
2. Singh AK, Ebenso EE, Quraishi M. Adsorption behaviour of cefapirin on mild steel in hydrochloric acid solution. *Int J Electrochem Sci.* 2012;(7):2320-33.
3. Chaouiki A, Lgaz H, Zehra S, et al. Exploring deep insights into the interaction mechanism of a quinazoline derivative with mild steel in HCl: electrochemical, DFT, and molecular dynamic simulation studies. *J Adhesion Sci Technol.* 2019;33(9):921-44. Doi: <https://doi.org/10.1080/01694243.2018.1554764>
4. Bouanis M, Tourabi M, Nyassi A, et al. Corrosion inhibition performance of 2, 5-bis (4-dimethylaminophenyl)-1, 3, 4-oxadiazole for carbon steel in HCl solution: Gravimetric, electrochemical and XPS studies. *Appl Surf Sci.* 2016;389:952–66. Doi: <https://doi.org/10.1016/j.apsusc.2016.07.115>
5. Kumar S, Udayabhanu G, John RP. 4 (N, N-dimethylamino) benzaldehyde nicotinic hydrazone as corrosion inhibitor for mild steel in 1 M HCl solution: An experimental and theoretical study. *J Mol Liq.* 2016;216:738–46. Doi: <https://doi.org/10.1016/j.molliq.2016.02.012>
6. Chaouiki A, Lgaz H, Salghi R., et al. Assessing the impact of electron-donating-substituted chalcones on inhibition of mild steel corrosion in HCl solution: Experimental results and molecular-level insights. *Colloids Surf A: Physicochem Eng Asp.* 2020;588:124366. Doi: <https://doi.org/10.1016/j.colsurfa.2019.124366>
7. Lgaz H, Saha SK, Chaouiki A, et al. Exploring the potential role of pyrallzoline derivatives in corrosion inhibition of mild steel in hydrochloric acid solution: Insights from experimental and computational studies. *Constr Building Mats.* 2020;233:117320. Doi: <https://doi.org/10.1016/j.conbuildmat.2019.117320>
8. Popova A, Christov M, Raicheva S, et al. Adsorption and inhibitive properties of benzimidazole derivatives in acid mild steel corrosion. *Corros Sci.* 2004;46 (6):1333–50. Doi: <https://doi.org/10.1016/j.corsci.2003.09.025>
9. Popova A, Christov M, Deligeorgiev T. Influence of the molecular structure on the inhibitor properties of benzimidazole derivatives on mild steel corrosion in 1 M hydrochloric acid. *Corr.* 2003;59(9):756–64. Doi: <https://doi.org/10.5006/1.3277604>
10. Wang X, Yang H, Wang F. An investigation of benzimidazole derivative as corrosion inhibitor for mild steel in different concentration HCl solutions.

- Corr Sci. 2011; 53(1):113–21. Doi: <https://doi.org/10.1016/j.corsci.2010.09.029>
11. Baviskar BA, Baviskar B, Shiradkar MR, et al. Synthesis and Antimicrobial Activity of Some Novel Benzimidazolyl Chalcones. *E-J Chem.* 2009;6(1):196–200. Doi: <https://doi.org/10.1155/2009/746292>
 12. Khaled KF. The inhibition of benzimidazole derivatives on corrosion of iron in 1 M HCl solutions. *Electrochim Acta.* 2003;48(17):2493–503. Doi: [https://doi.org/10.1016/S0013-4686\(03\)00291-3](https://doi.org/10.1016/S0013-4686(03)00291-3)
 13. Abboud Y, Abourriche A, Saffaj T, et al. The inhibition of mild steel corrosion in acidic medium by 2, 2'-bis (benzimidazole). *Appl Surf Sci.* 2006;252(23):8178–84. Doi: <https://doi.org/10.1016/j.apsusc.2005.10.060>
 14. Aljourani J, Raeissi K, Golozar MA. Benzimidazole and its derivatives as corrosion inhibitors for mild steel in 1M HCl solution. *Corr Sci.* 2009;51(8):1836–43. Doi: <https://doi.org/10.1016/j.corsci.2009.05.011>
 15. Popova A, Christov M. Evaluation of impedance measurements on mild steel corrosion in acid media in the presence of heterocyclic compounds. *Corr Sci.* 2006;48(10):3208–21. Doi: <https://doi.org/10.1016/j.corsci.2005.11.001>
 16. Popova A, Sokolova E, Raicheva S, et al. AC and DC study of the temperature effect on mild steel corrosion in acid media in the presence of benzimidazole derivatives. *Corr Sci.* 2003;45(1):33–58. Doi: [https://doi.org/10.1016/S0010-938X\(02\)00072-0](https://doi.org/10.1016/S0010-938X(02)00072-0)
 17. Popova A, Christov M, Zwetanova A. Effect of the molecular structure on the inhibitor properties of azoles on mild steel corrosion in 1 M hydrochloric acid. *Corros Sci.* 2007;49(5):2131–43. Doi: <https://doi.org/10.1016/j.corsci.2006.10.021>
 18. Aljourani J, Golozar MA, Raeissi K. The inhibition of carbon steel corrosion in hydrochloric and sulfuric acid media using some benzimidazole derivatives. *Mat Chem Phys.* 2010;121(1):320–5. Doi: <https://doi.org/10.1016/j.matchemphys.2010.01.040>
 19. Zhang Z, Tian N, Huang X, et al. Synergistic inhibition of carbon steel corrosion in 0.5 M HCl solution by indigo carmine and some cationic organic compounds: experimental and theoretical studies. *RSC Advances.* 2016;6(27):22250–68. Doi: <https://doi.org/10.1039/C5RA25359D>
 20. Ezeoke AU, Adeyemi OG, Akerele OA, et al. Computational and experimental studies of 4-aminoantipyrine as corrosion inhibitor for mild steel in sulphuric acid solution. *Int. J. Electrochem. Sci.* 2012;7:534–53.
 21. Wang HL, Fan HB, Zheng JS. Corrosion inhibition of mild steel in hydrochloric acid solution by a mercapto-triazole compound. *Mat Chem Phys.* 2003;77(3):655–61. Doi: [https://doi.org/10.1016/S0254-0584\(02\)00123-2](https://doi.org/10.1016/S0254-0584(02)00123-2)
 22. Zhang QB, Hua YX. Corrosion inhibition of mild steel by alkylimidazolium ionic liquids in hydrochloric acid. *Electrochim Acta.* 2009;54(6):1881–7. Doi: <https://doi.org/10.1016/j.electacta.2008.10.025>
 23. Bentiss F, Lebrini M, Vezin H, et al. Experimental and theoretical study of 3-pyridyl-substituted 1, 2, 4-thiadiazole and 1, 3, 4-thiadiazole as corrosion

- inhibitors of mild steel in acidic media. *Mat Chem Phys.* 2004;87(1):18–23. Doi: <https://doi.org/10.1016/j.matchemphys.2004.05.040>
24. Verma CB, Quraishi M, Singh A. 2-Aminobenzene-1, 3-dicarbonitriles as green corrosion inhibitor for mild steel in 1 M HCl: Electrochemical, thermodynamic, surface and quantum chemical investigation. *J Taiwan Inst Chem Eng.* 2015;49:229–39. Doi: <https://doi.org/10.1016/j.jtice.2014.11.029>
25. Quraishi M, Sardar R, Jamal D. Corrosion inhibition of mild steel in hydrochloric acid by some aromatic hydrazides. *Mat Chem Phys.* 2001;71(3): 309–13. Doi: [https://doi.org/10.1016/S0254-0584\(01\)00295-4](https://doi.org/10.1016/S0254-0584(01)00295-4)
26. Bentiss F, Lagrenée M, Traisnel M, et al. The corrosion inhibition of mild steel in acidic media by a new triazole derivative. *Corros Sci.* 1999;41(4):789–803. Doi: [https://doi.org/10.1016/S0010-938X\(98\)00153-X](https://doi.org/10.1016/S0010-938X(98)00153-X)
27. Ferreira ES, Giacomelli C, Giacomelli FC, et al. Evaluation of the inhibitor effect of L-ascorbic acid on the corrosion of mild steel. *Mater Chem Phys.* 2004;83(1):129–134. Doi: <https://doi.org/10.1016/j.matchemphys.2003.09.020>
28. de Souza FS, Spinelli A. Caffeic acid as a green corrosion inhibitor for mild steel. *Corros Sci.* 2009;51(3):642–9. Doi: <https://doi.org/10.1016/j.corsci.2008.12.013>
29. Ashassi-Sorkhabi H, Shaabani B, Seifzadeh D. Corrosion inhibition of mild steel by some Schiff base compounds in hydrochloric acid. *Appl Surf Sci.* 2005;239(2):154–64. Doi: <https://doi.org/10.1016/j.apsusc.2004.05.143>
30. Lebrini M, Robert F, Roos C. Inhibition effect of alkaloids extract from *Annona squamosa* plant on the corrosion of C38 steel in normal hydrochloric acid medium. *Int J Electrochem Sci.* 2010;5(11):1698–712.
31. Tang Y, Zhang F, Hu S, et al. Novel benzimidazole derivatives as corrosion inhibitors of mild steel in the acidic media. Part I: gravimetric, electrochemical, SEM and XPS studies. *Corros Sci.* 2013;74:271–82. Doi: <https://doi.org/10.1016/j.corsci.2013.04.053>
32. Daoud D, Douadi T, Hamani H, et al. Corrosion inhibition of mild steel by two new S-heterocyclic compounds in 1 M HCl: experimental and computational study. *Corros Sci.* 2015;94:21–37. Doi: <https://doi.org/10.1016/j.corsci.2015.01.025>
33. Fragoza-Mar L, Olivares-Xometl O, Domínguez-Aguilar, et al. Corrosion inhibitor activity of 1, 3-diketone malonates for mild steel in aqueous hydrochloric acid solution. *Corros Sci.* 2012;61:171–84. Doi: <https://doi.org/10.1016/j.corsci.2012.04.031>
34. Oguzie EE. Evaluation of the inhibitive effect of some plant extracts on the acid corrosion of mild steel. *Corros Sci.* 2008;50(11):2993–8. Doi: <https://doi.org/10.1016/j.corsci.2008.08.004>
35. Ramesh SV, Adhikari AV. Corrosion inhibition of mild steel in acid media by quinolinyl thiopropano hydrazone. *Indian J Chem Techn.* 2009;16(2):162–74.
36. Wang X, Yang H, Wang F. A cationic gemini-surfactant as effective inhibitor for mild steel in HCl solutions. *Corros Sci.* 2010;52(4):1268–76. Doi: <https://doi.org/10.1016/j.corsci.2009.12.018>

37. Migahed MA. Electrochemical investigation of the corrosion behaviour of mild steel in 2M HCl solution in presence of 1-dodecyl-4-methoxy pyridinium bromide. *Mater Chem Phys.* 2005;93(1):48–53. Doi: <https://doi.org/10.1016/j.matchemphys.2005.02.003>
38. Fouda AS, Heakal FE, Radwan MS. Role of some thiadiazole derivatives as inhibitors for the corrosion of C-steel in 1 M H₂SO₄. *J Appl Electrochem.* 2009;39(3):391–402. Doi: <https://doi.org/10.1007/s10800-008-9684-2>
39. Behpour M, Ghoreishi SM, Soltani N, et al. Electrochemical and theoretical investigation on the corrosion inhibition of mild steel by thiosalicylaldehyde derivatives in hydrochloric acid solution. *Corros Sci.* 2008;50 (8):2172–81. Doi: <https://doi.org/10.1016/j.corsci.2008.06.020>
40. Ehsani A, Mahjani MG, Moshrefi R. Electrochemical and DFT study on the inhibition of 316L stainless steel corrosion in acidic medium by 1-(4-nitrophenyl)-5-amino-1 H-tetrazole. *RSC Adv.* 2014;4(38):20031–7. Doi: <https://doi.org/10.1039/C4RA01029A>
41. Dutta A, Saha SK, Banerjee P, et al. Evaluating corrosion inhibition property of some Schiff bases for mild steel in 1 M HCl: competitive effect of the heteroatom and stereochemical conformation of the molecule. *RSC Adv.* 2016;6(78): 74833–44. Doi: <https://doi.org/10.1039/C6RA03521C>
42. Fu J, Zang H, Wang Y, et al. Experimental and theoretical study on the inhibition performances of quinoxaline and its derivatives for the corrosion of mild steel in hydrochloric acid. *Industr Eng Chem Research.* 2012;51(18):6377–86. Doi: <https://doi.org/10.1021/ie202832e>
43. Obot I, Gasem Z, Umoren S. Molecular level understanding of the mechanism of aloes leaves extract inhibition of low carbon steel corrosion: a DFT approach. *Int. J. Electrochem. Sci.* 2014;9:510–22.
44. Pearson RG. Absolute electronegativity and hardness: application to inorganic chemistry. *Inorg Chem.* 1988;27(4):734–40. Doi: <https://doi.org/10.1021/ic00277a030>
45. Sastri V, Perumareddi J. Molecular orbital theoretical studies of some organic corrosion inhibitors. *Corrosion.* 1997;53(8):617–22. Doi: <https://doi.org/10.5006/1.3290294>
46. Kokalj A. On the HSAB based estimate of charge transfer between adsorbates and metal surfaces. *Chem Physics.* 2012;393(1):1–12. Doi: <https://doi.org/10.1016/j.chemphys.2011.10.021>
47. Saha SK, Murmu M, Murmu NC, et al. Evaluating electronic structure of quinazolinone and pyrimidinone molecules for its corrosion inhibition effectiveness on target specific mild steel in the acidic medium: A combined DFT and MD simulation study. *J Mol Liq.* 2016;224:629–38. Doi: <https://doi.org/10.1016/j.molliq.2016.09.110>
48. Xia S, Qiu M, Yu L, et al. Molecular dynamics and density functional theory study on relationship between structure of imidazoline derivatives and inhibition performance. *Corros Sci.* 2008;50 (7):2021–9. Doi: <https://doi.org/10.1016/j.corsci.2008.04.021>

49. Obot I, Gasem Z. Theoretical evaluation of corrosion inhibition performance of some pyrazine derivatives. *Corros Sci.* 2014;83:359–66. Doi: <https://doi.org/10.1016/j.corsci.2014.03.008>
50. Dutta A, Saha SK, Banerjee P, et al. Evaluating corrosion inhibition property of some Schiff bases for mild steel in 1 M HCl: competitive effect of the heteroatom and stereochemical conformation of the molecule. *RSC Adv.* 2016;6(78): 74833–44. Doi: <https://doi.org/10.1039/C6RA03521C>
51. Gao G, Liang C. Electrochemical and DFT studies of β -amino-alcohols as corrosion inhibitors for brass. *Electrochim Acta.* 2007;52(13):4554–9. Doi: <https://doi.org/10.1016/j.electacta.2006.12.058>
52. Kokalj A. Is the analysis of molecular electronic structure of corrosion inhibitors sufficient to predict the trend of their inhibition performance. *Electrochim Acta.* 2010;56(2):745–55. Doi: <https://doi.org/10.1016/j.electacta.2010.09.065>
53. KovaAeeviAe N, Kokalj A. Analysis of molecular electronic structure of imidazole- and benzimidazole-based inhibitors: A simple recipe for qualitative estimation of chemical hardness. *Corros Sci.* 2011;53(3):909–21. Doi: <https://doi.org/10.1016/j.corsci.2010.11.016>
54. Awad MK, Mustafa MR, Elnga, MMA. Computational simulation of the molecular structure of some triazoles as inhibitors for the corrosion of metal surface. *J Mol Struct: Theochem.* 2010;959(1):66–74. Doi: <https://doi.org/10.1016/j.theochem.2010.08.008>
55. Yadav DK, Maiti B, Quraishi M. Electrochemical and quantum chemical studies of 3, 4-dihydropyrimidin-2 (1H)-ones as corrosion inhibitors for mild steel in hydrochloric acid solution. *Corros Sci.* 2010;52 (11):3586–98. Doi: <https://doi.org/10.1016/j.corsci.2010.06.030>
56. Obot I, Gasem Z. Theoretical evaluation of corrosion inhibition performance of some pyrazine derivatives. *Corros Sci.* 2014;83:359–66. Doi: <https://doi.org/10.1016/j.corsci.2014.03.008>
57. Obot I, Umoren S, Gasem Z, et al. Theoretical prediction and electrochemical evaluation of vinylimidazole and allylimidazole as corrosion inhibitors for mild steel in 1M HCl. *J Ind Eng Chem.* 2015;21:1328–39. Doi: <https://doi.org/10.1016/j.jiec.2014.05.049>